Supporting Information

Experimental and Theoretical Studies of a Pyridylvinyl(benzoate) Based Coordination Polymer Structure

Yuri Dezotti,[a] Manoel Victor Frutuoso Barrionuevo,[a] Ingrid Fernandes Silva,[b] Marcos Antônio Ribeiro,[c] Rafael Añez,[d] Humberto Osório Stumpf,[b] Miguel Angel San-Miguel,[a] Wdeson Pereira Barros[a]**

[a]Instituto de Química, Universidade Estadual de Campinas, SP 13083-970, Brazil

[b]Departamento de Química, ICEx, Universidade Federal de Minas Gerais, Av. Antônio Carlos 6627, Belo Horizonte, MG, 31270-901, Brazil

[c]Departamento de Química, Universidade Federal do Espírito Santo,Vitória, ES 29075-910, Brazil.

[d]Laboratorio de Química Física y Catálisis Computacional, Centro de Química, Instituto Venezolano de Investigaciones Científicas, Caracas 21827, Venezuela.

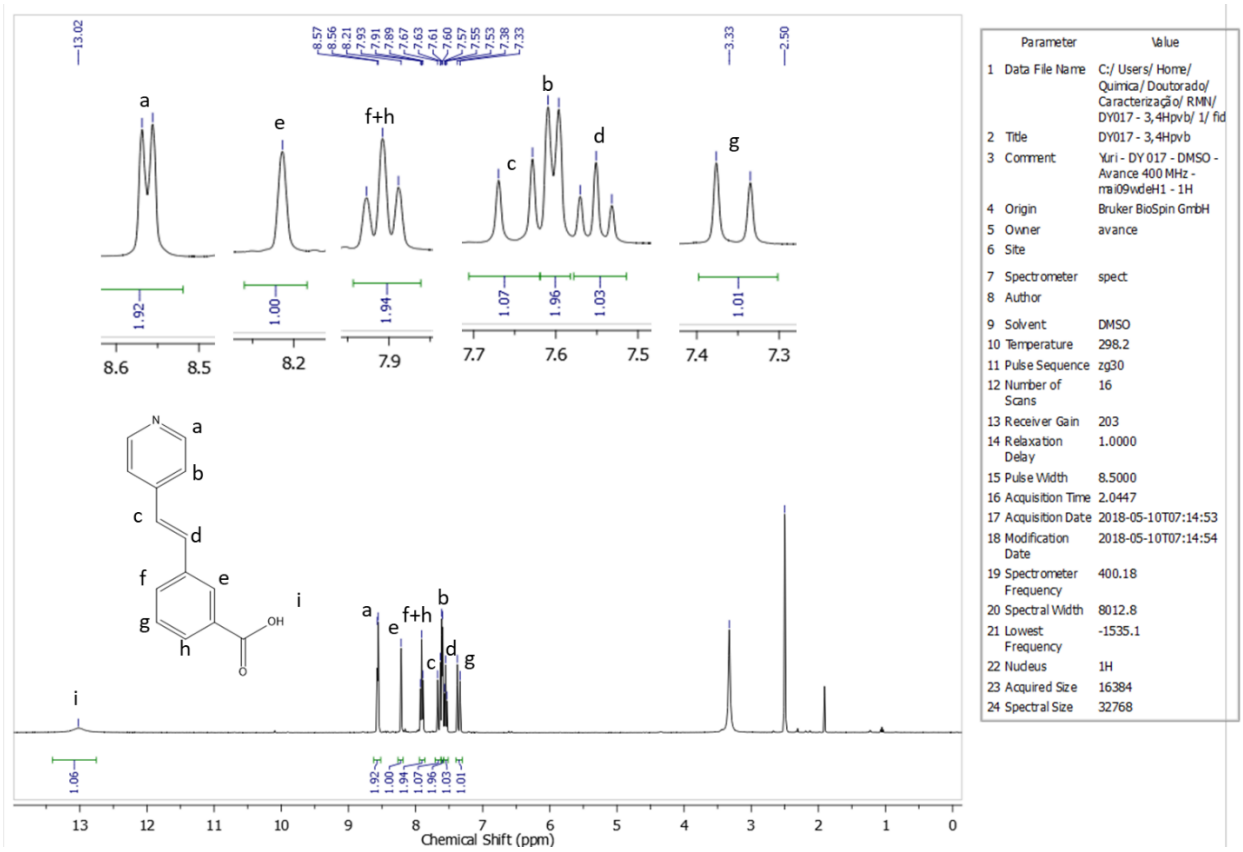

Figure S1. ^{1}H NMR spectrum in dmso-d_6 for the **3,4-Hpvb**.

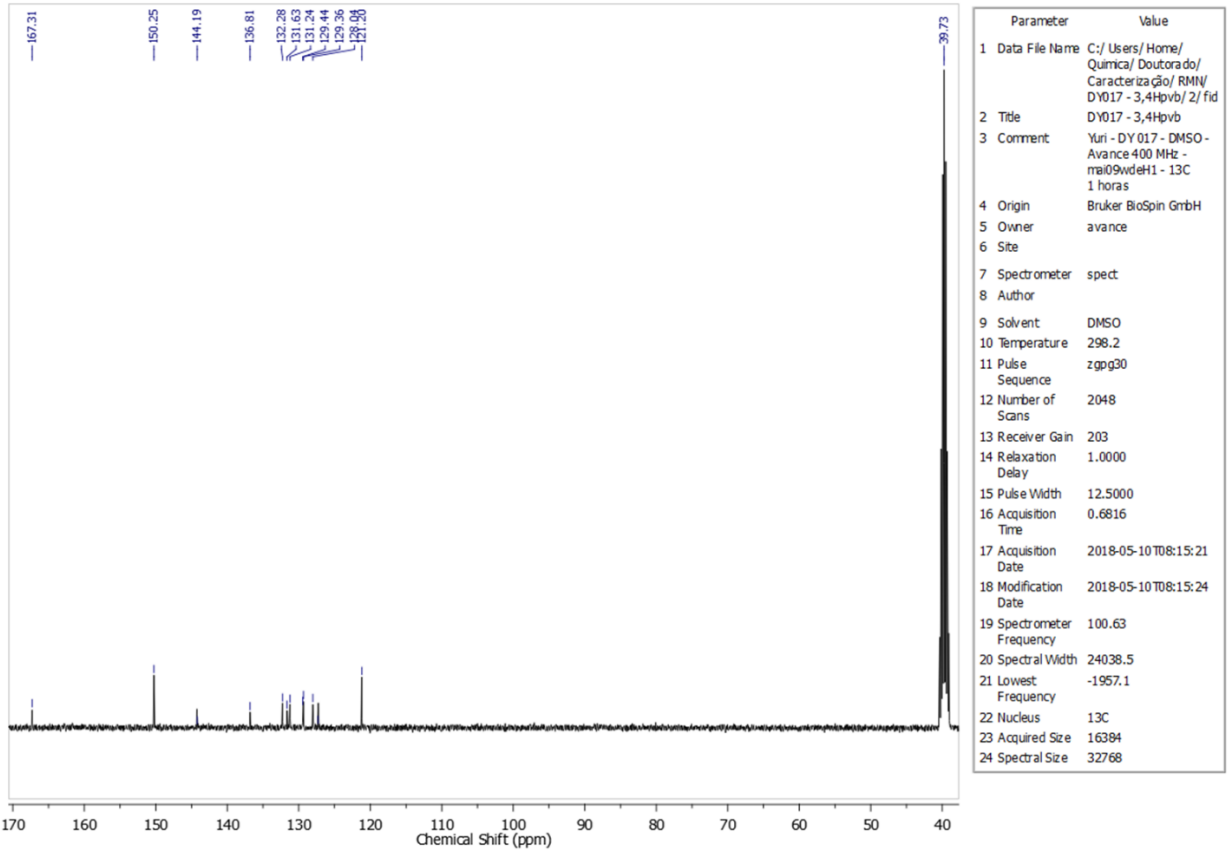

	Parameter	Value
1	Data File Name	C:/ Users/ Home/ Quimica/ Doutorado/ Caracterização/ RMN/ DY017 - 3,4Hpvb/ 2/ fid
2	Title	DY017 - 3,4Hpvb
3	Comment	Yuri - DY 017 - DMSO - Avance 400 MHz - rmai09wdeH1 - 13C 1 horas
4	Origin	Bruker BioSpin GmbH
5	Owner	avance
6	Site	
7	Spectrometer	spect
8	Author	
9	Solvent	DMSO
10	Temperature	298.2
11	Pulse Sequence	zgpg30
12	Number of Scans	2048
13	Receiver Gain	203
14	Relaxation Delay	1.0000
15	Pulse Width	12.5000
16	Acquisition Time	0.6816
17	Acquisition Date	2018-05-10T08:15:21
18	Modification Date	2018-05-10T08:15:24
19	Spectrometer Frequency	100.63
20	Spectral Width	24038.5
21	Lowest Frequency	-1957.1
22	Nucleus	13C
23	Acquired Size	16384
24	Spectral Size	32768

Figure S2. ^{13}C NMR spectrum in dmso-d_6 for the **3,4-Hpvb**.

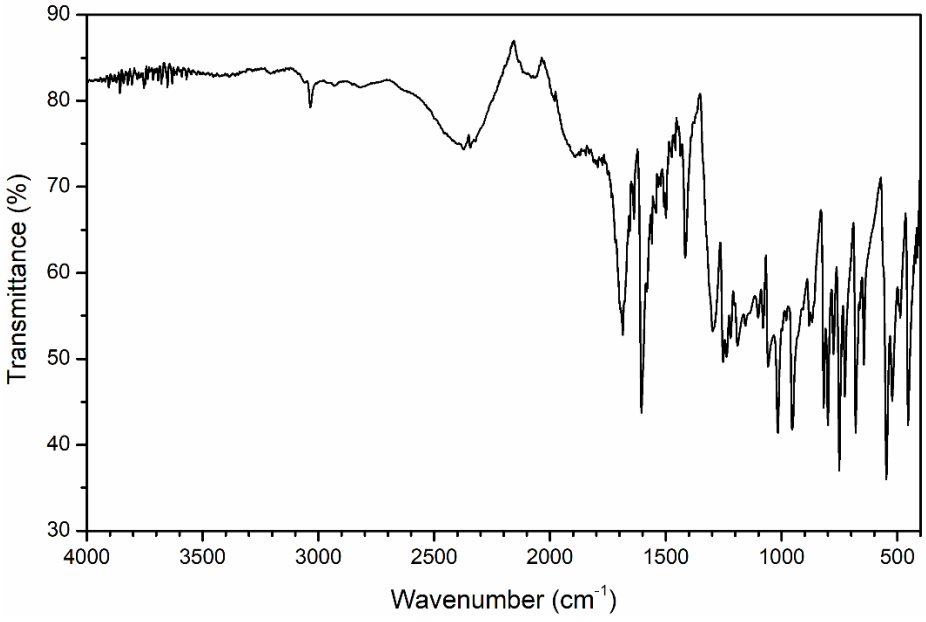

Figure S3. FT-IR (ATR) spectrum for the **3,4-Hpvb**.

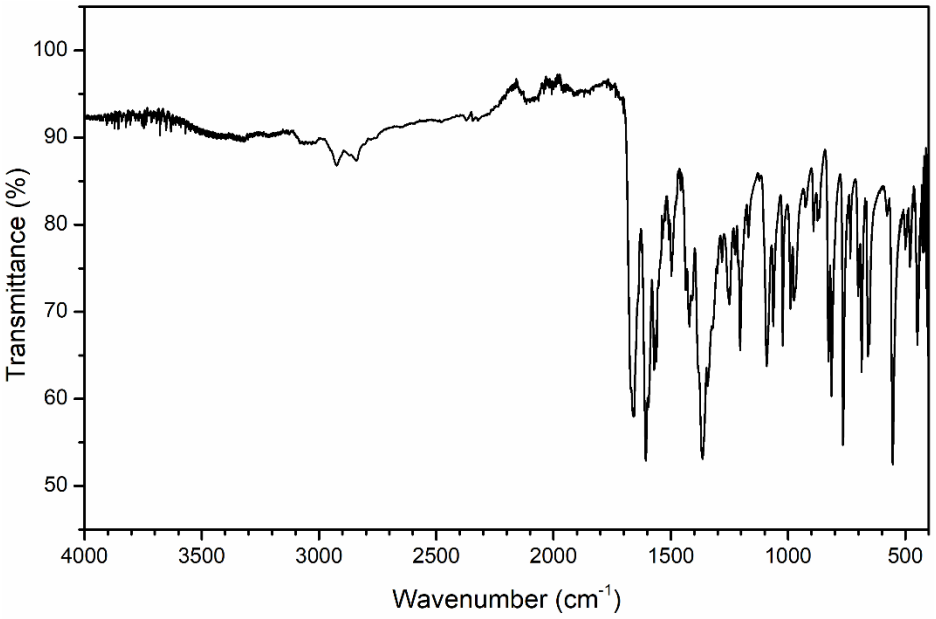

Figure S4. FT-IR (ATR) spectrum for compound **1**.

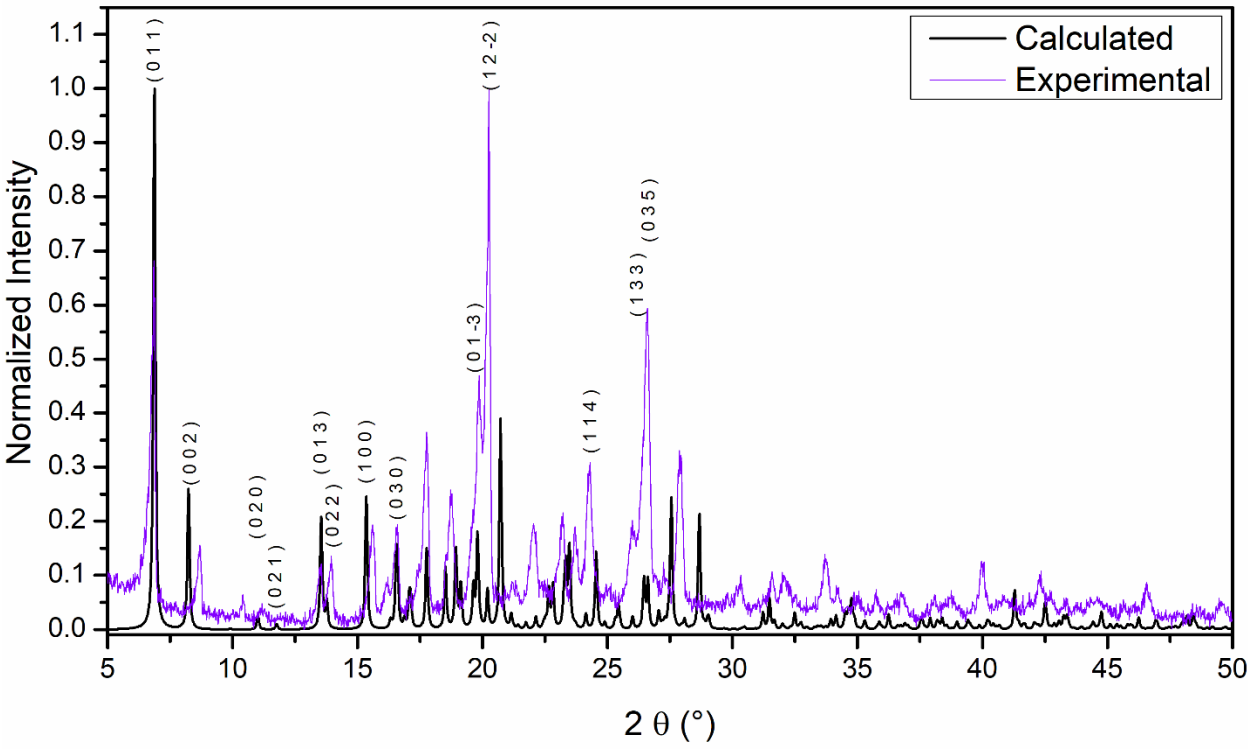

Figure S5. Experimental and calculated PXRD pattern for compound **1**. Some (hkl) reflection indexes from the calculated PXRD pattern are shown for comparison.

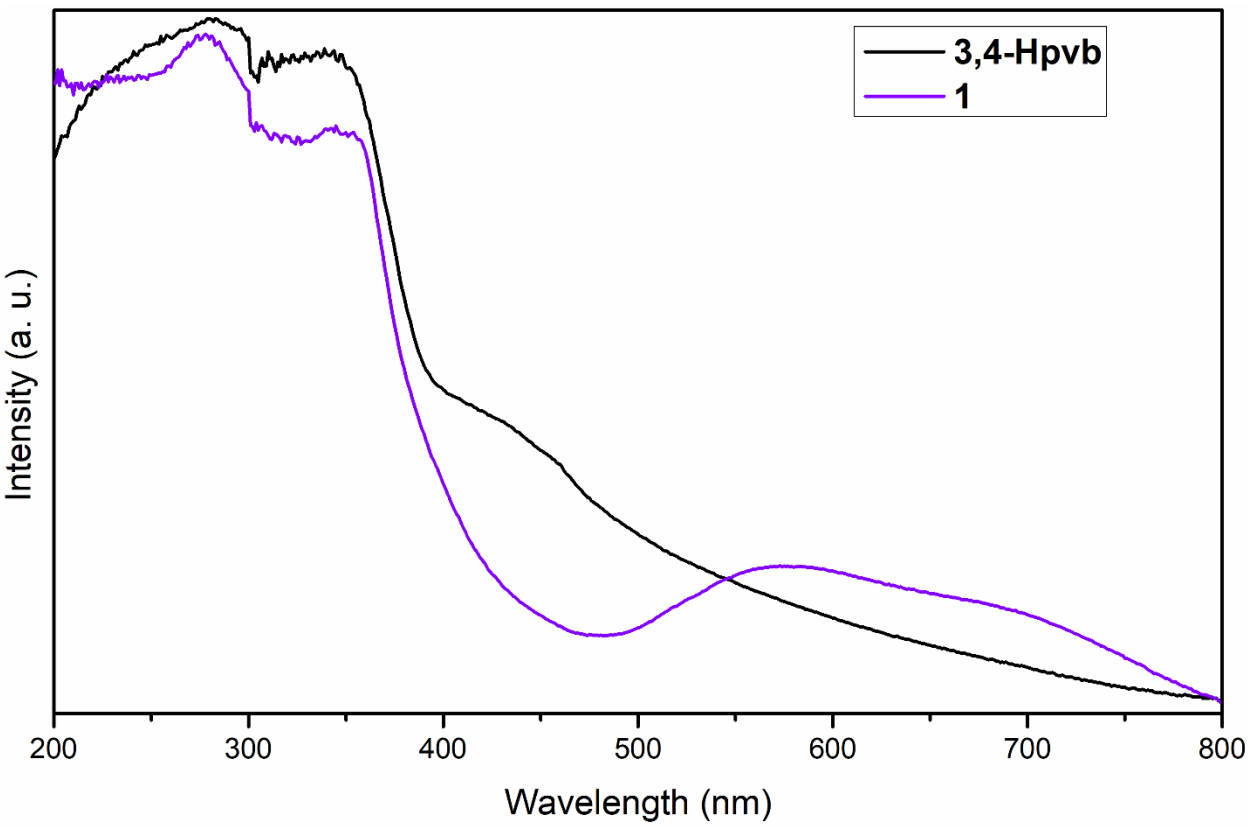

Figure S6. Electronic spectra obtained by the DRS method for the **3,4-Hpvb** pre-ligand (black line), with λ_{max} around 280, 350, and 440 nm, characteristic of intra-ligand transitions, and for compound **1** (blue line), with λ_{max} around 580 and 700 nm, characteristic of d-d transitions.

Table S1. Continuous Shape Measures (CShM) analysis for compound **1**.

Coordination number	SHAPE label	Reference Polyhedra	Symmetry	CShM value[a]
4	SP-4	Square	D_{4h}	0.06008
	T4	Tetrahedron	T_d	33.37338
	SS-4	Seesaw	C_{2v}	18.41743
	vTBPY-4	Axially vacant trigonal bipyramid	C_{3v}	34.59204
6	HP-6	Hexagon	D_{6h}	22.64759
	PPY-6	Pentagonal pyramid	C_{5v}	26.43905
	OC-6	Octahedron	O_h	8.57224
	TPR-6	Trigonal prism	D_{3h}	19.43249
	JPPY-6	Johnson pentagonal pyramid (J2)	C_{5v}	26.92323

[a] The smallest value indicates proximity between the actual coordination sphere and the idealized polyhedron.

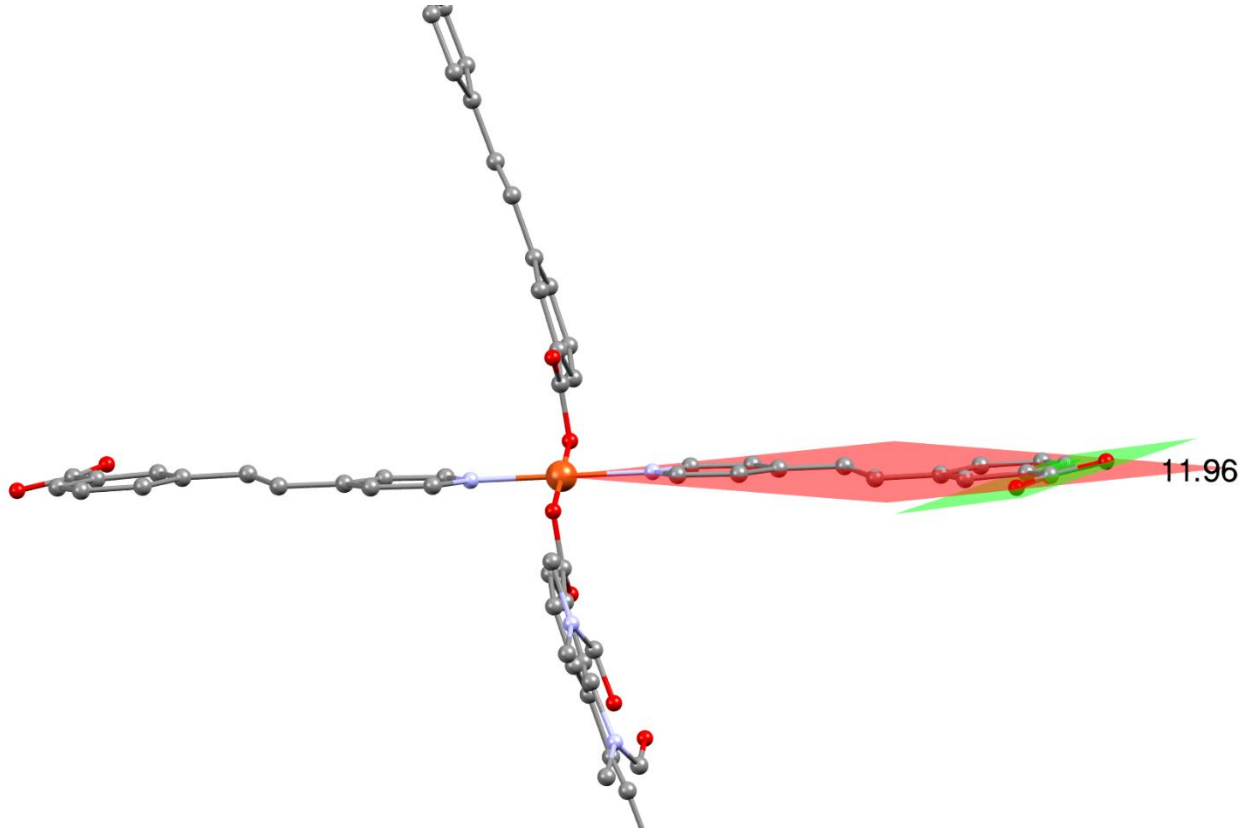

Figure S7. Angle between the **3,4-pvb**$^{-}$ mean-plane and the carboxylate mean-plane. Pink plane: C2 C3 C4 C5 C6 C7 C8 C9 C10 C11 C12 C13 C14 N1 O1 O2 C1; Rms of fitted atoms: 0.1015. Green plane: O1 O2 C1; Rms of fitted atoms: 0.0.

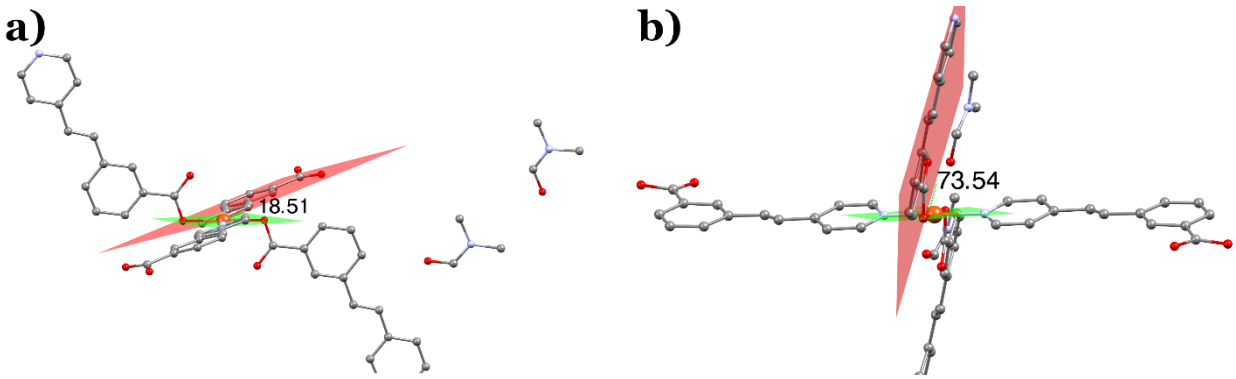

Figure S8. Angle between the **3,4-pvb**$^{-}$ mean-plane and the copper(II) basal plane. a) Green plane: O2 $O2^{iii}$ $N1^{i}$ $N1^{ii}$; Rms of fitted atoms: 0.0. Pink plane: $C2^{i}$ $C3^{i}$ $C4^{i}$ $C5^{i}$ $C6^{i}$ $C7^{i}$ $C8^{i}$ $C9^{i}$ $C10^{i}$ $C11^{i}$ $C12^{i}$ $C13^{i}$ $C14^{i}$ $N1^{i}$ $O1^{i}$ $O2^{i}$ $C1^{i}$; Rms of fitted atoms: 0.1015. b) Green plane: O2 $O2^{iii}$ $N1^{i}$ $N1^{ii}$; Rms of fitted atoms: 0.0. Pink plane: $C2^{iii}$ $C3^{iii}$ $C4^{iii}$ $C5^{iii}$ $C6^{iii}$ $C7^{iii}$ $C8^{iii}$ $C9^{iii}$ $C10^{iii}$ $C11^{iii}$ $C12^{iii}$ $C13^{iii}$ $C14^{iii}$ $N1^{iii}$ $O1^{iii}$ $O2^{iii}$ $C1^{iii}$; Rms of fitted atoms: 0.1015.

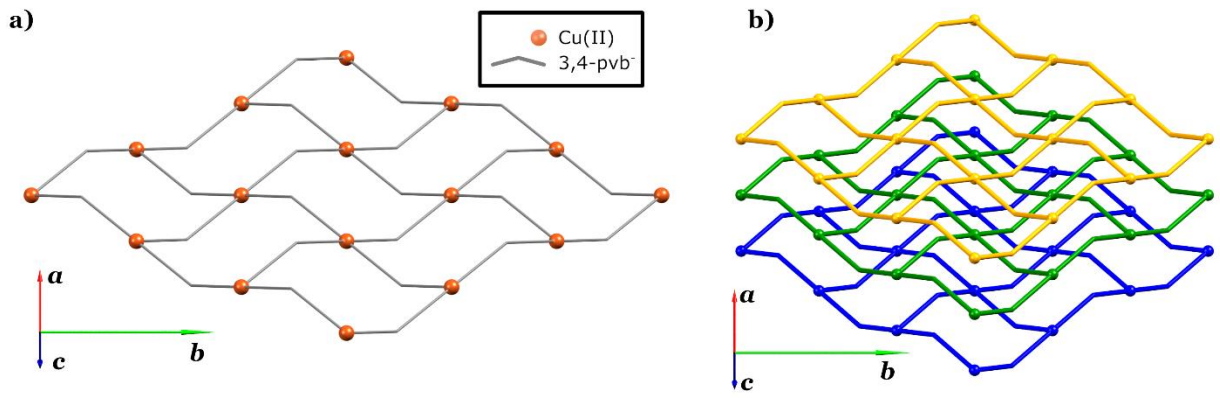

Figure S9. Simplified molecular structure of {[Cu(**3,4-pvb**)$_2$]·4(dmf)}$_n$ showing a) arrangement between the 4-connected metal nodes and the **3,4-pvb**$^-$ bridges in one corrugated layer; (b) overall three-dimensional supramolecular structure of {[Cu(**3,4-pvb**)$_2$]·4(dmf)}$_n$ with the parallel stacking of the corrugated layers. Solvent molecules are not shown for clarity purposes.

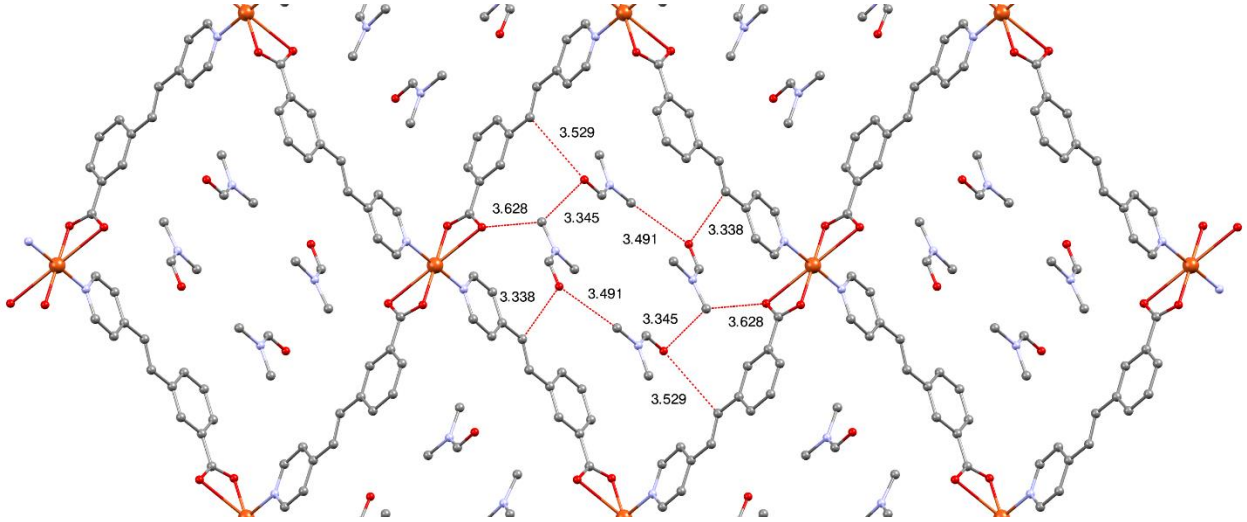

Figure S10. Intermolecular interactions between dmf molecules and the **3,4-pvb**$^-$ moieties (view along the *a*-axis).

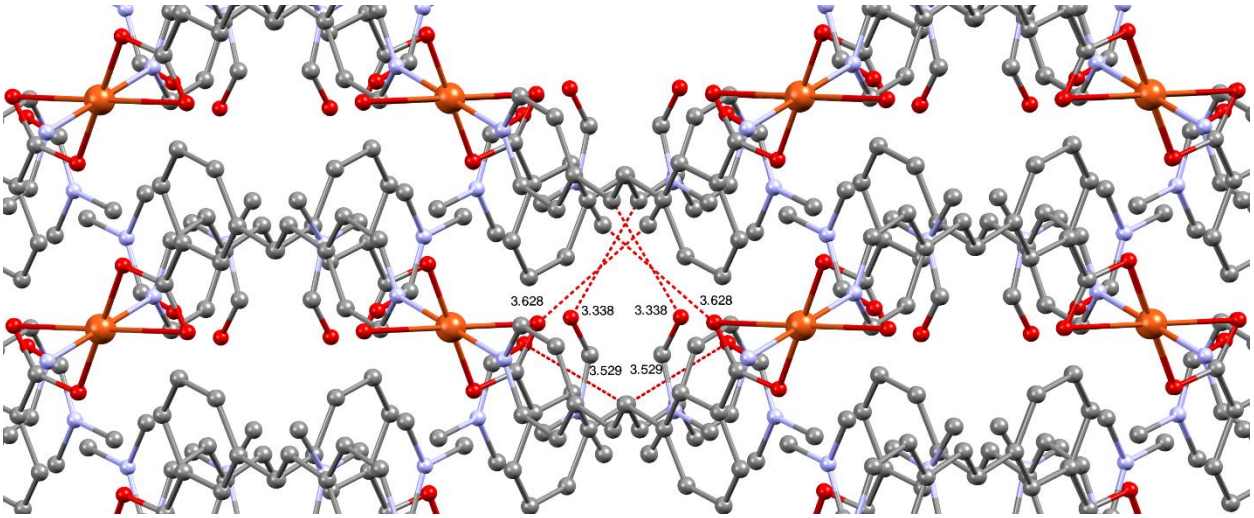

Figure S11. Intermolecular interactions between dmf molecules and the **3,4-pvb**$^{-}$ moieties.

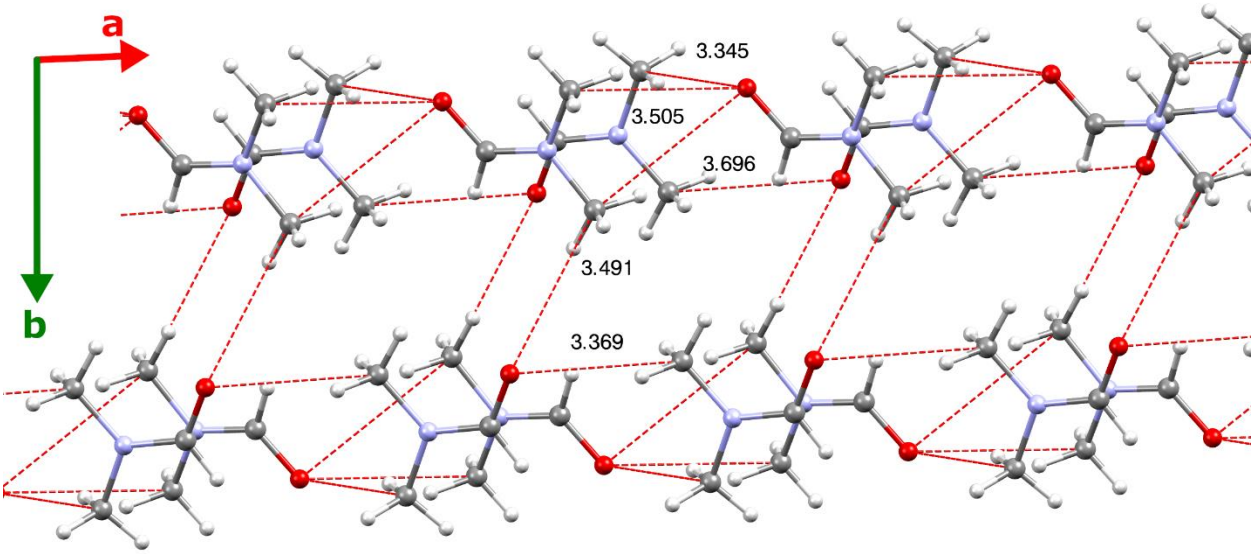

Figure S12. Intermolecular interactions between dmf molecules across one rhombus channel (only dmf molecules are shown for the sake of clarity).

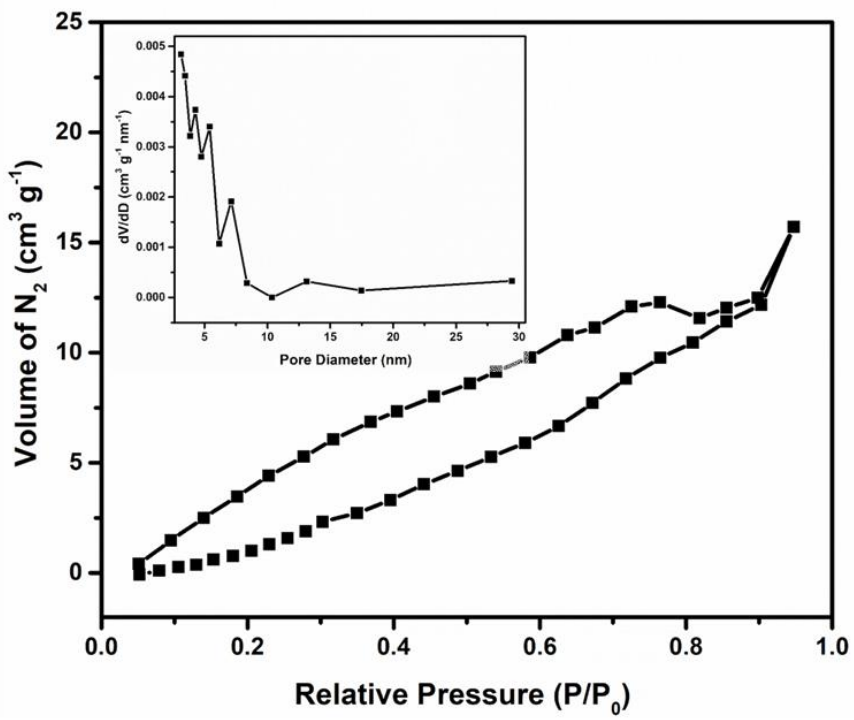

Figure S13. N_2 adsorption-desorption isotherm pattern for **1**. Insert: Pore size distribution calculated from the N_2 adsorption-desorption isotherm by the BJH method.

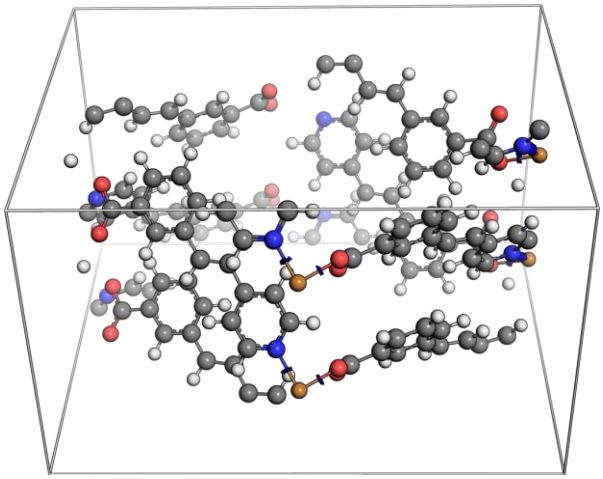

Figure S14. NCI isosurface (0.3 bohr) representation for the first domain.

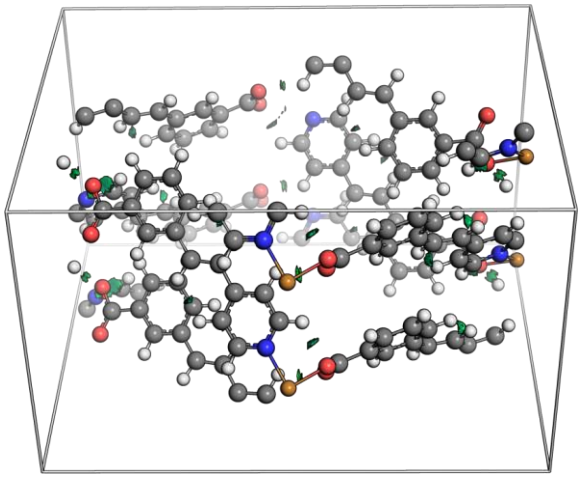

Figure S15. NCI isosurface (0.3 bohr) representation for the second domain.

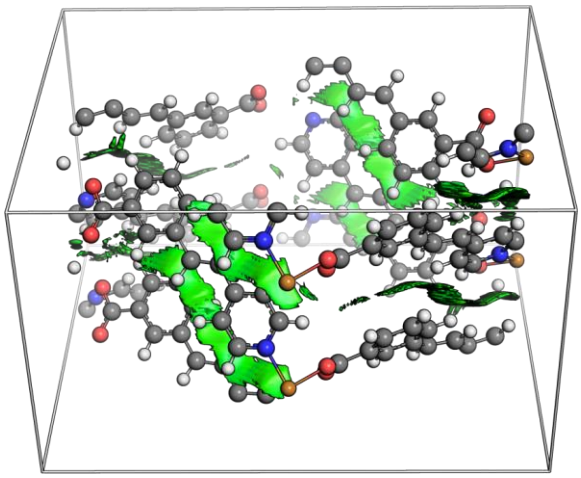

Figure S16. NCI isosurface (0.3 bohr) representation for the third domain.

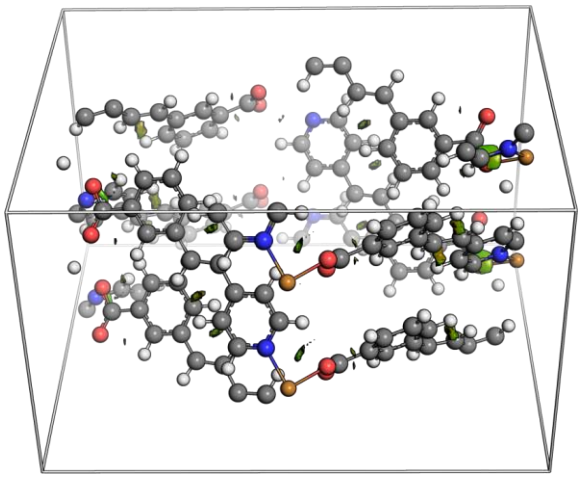

Figure S17. NCI isosurface (0.3 bohr) representation for the fourth domain.

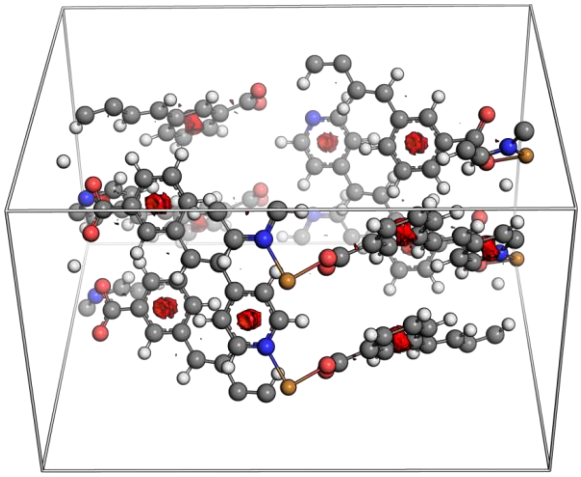

Figure S18. NCI isosurface (0.3 bohr) representation for the fifth domain.

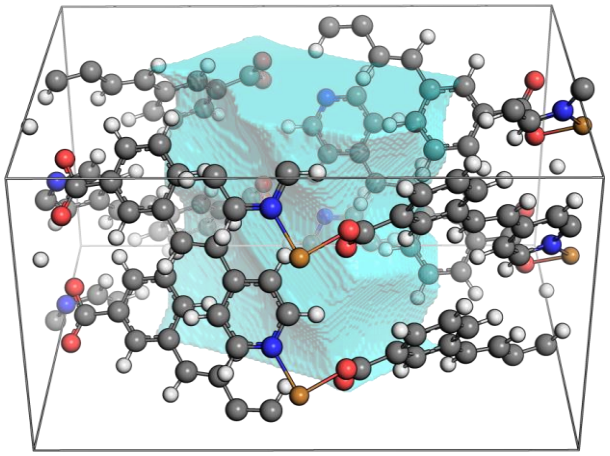

Figure S19. Isosurface volume for the central cavity pore highlighted for clarity.

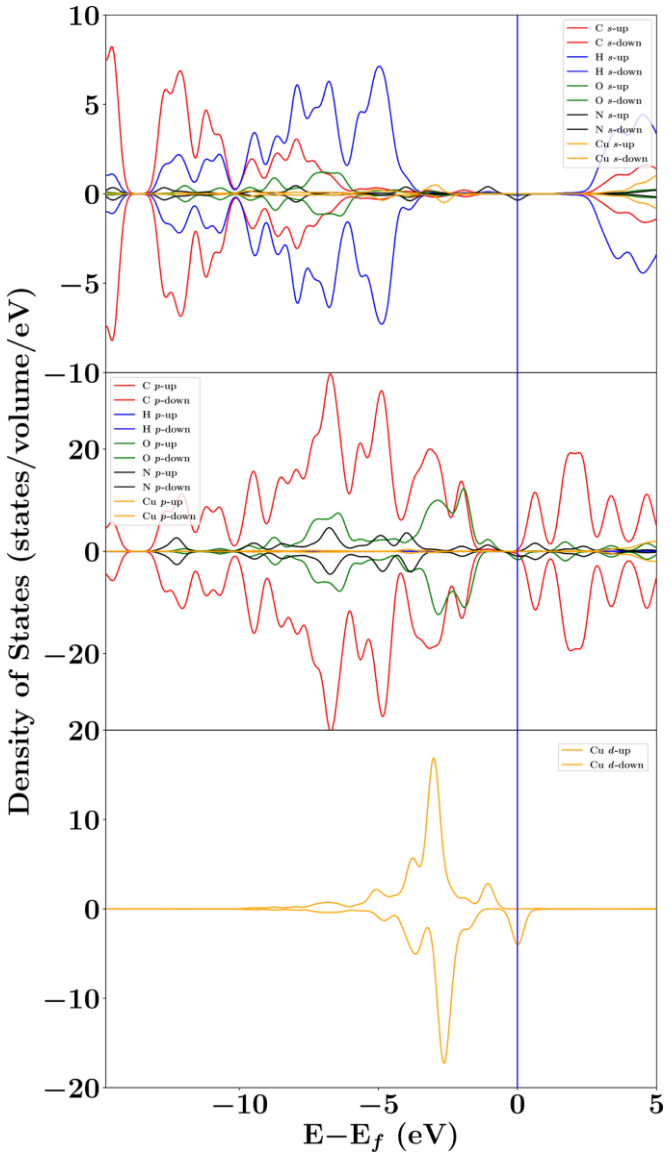

Figure S20. PDOS for *s*, *p* and *d* states for each atomic specie.

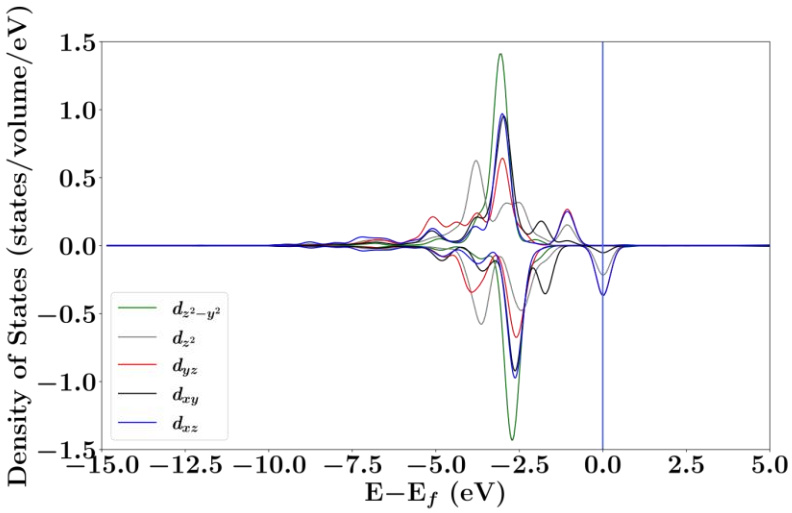

Figure S21 PDOS for *d*-states of copper(II) upon coordination with 4 ligands of **3,4-pvb**$^-$.